The Astrophysical Journal Letters, 883:L3 (6pp), 2019 September 20 https://doi.org/10.3847/2041-8213/ab3e09

A Simple Phenomenological Emergent Dark Energy Model can Resolve the Hubble Tension

Xiaolei Li[1,2] and Arman Shafieloo[1,3]
[1] Korea Astronomy and Space Science Institute, Daejeon 34055, Republic of Korea
[2] Quantum Universe Center, Korean Institute of Advanced Studies, Hoegiro 87, Dongdaemun-gu, Seoul 130-722, Republic of Korea
[3] University of Science and Technology, Yuseong-gu 217 Gajeong-ro, Daejeon 34113, Republic of Korea
Received 2019 July 8; revised 2019 August 20; accepted 2019 August 23; published 2019 September 17

Abstract

Motivated by the current status of cosmological observations and significant tensions in the estimated values of some key parameters assuming the standard ΛCDM model, we propose a simple but radical phenomenological emergent dark energy model where dark energy has no effective presence in the past and emerges at later times. Theoretically, in this phenomenological dark energy model with zero degrees of freedom (similar to a ΛCDM model), one can derive that the equation of state of dark energy increases from $-\frac{2}{3\ln 10} - 1$ in the past to -1 in the future. We show that by setting a hard-cut 2σ lower bound prior for H_0 associated with a 97.72% probability from recent local observations, this model can satisfy different combinations of cosmological observations at low and high redshifts (SNe Ia, baryon acoustic oscillation (BAO), Lyα BAO, and cosmic microwave background (CMB)) substantially better than the concordance ΛCDM model with $\Delta\chi^2_{bf} \sim -41.08$ and Δ DIC ~ -35.38. If there are no substantial systematics in SN Ia, BAO, or *Planck* CMB data, and assuming the reliability of current local H_0 measurements, there is a very high probability that with more precise measurements of the Hubble constant our proposed phenomenological model rules out the cosmological constant with decisive statistical significance and is a strong alternative to explain the combination of different cosmological observations. This simple phenomenologically emergent dark energy model can guide theoretically motivated dark energy model building activities.

Unified Astronomy Thesaurus concepts: Hubble constant (758); Cosmological parameters (339); Dark energy (351); Cosmological constant (334); Observational cosmology (1146)

1. Introduction

While current cosmological observations have been in great agreement with the standard ΛCDM model, there is significant tension regarding the estimation of some key cosmological parameters derived by assuming this model. One of the major issues is the inconsistency between the local measurement of the Hubble constant by the *Supernova H0 for the Equation of State* (*SH0ES*) collaboration (Riess et al. 2016, 2018, 2019) and the estimation of this parameter using *Planck* cosmic microwave background (CMB) and other cosmological observations assuming the ΛCDM model (Ade et al. 2016; Aghanim et al. 2018). Another issue is the estimation of the $\Omega_m h_0^2$ from the baryon acoustic oscillation (BAO) measurement at $z = 2.34$ from the BOSS and eBOSS surveys using the Lyα forest and estimated values from *Planck* CMB observations assuming the ΛCDM model (Sahni et al. 2014; Ding et al. 2015; Zheng et al. 2016; Alam et al. 2017b; Solà et al. 2017; Shanks et al. 2019).

A possible solution to these issues may be a carefully constructed yet simple alternative model of dark energy that can satisfy all of the observations, or an unconventional model of the early universe (Hazra et al. 2019).

In this Letter we propose a simple (zero degrees of freedom) but radical phenomenological model of dark energy with symmetrical behavior around the current time where dark energy and matter densities are comparable. In this model dark energy has no effective presence in the past, and emerges at later times. Setting hard-cut priors from local measurements of the Hubble constant, we confront this model with a combination of low- and high-redshift cosmological observations, namely SNe Ia data, BAO data (including BAO Lyα measurements), and CMB measurements, and show that statistically it can outperform the standard ΛCDM model as well as the w_0–w_a parameterization.

This Letter is organized as follows. In Section 2 we briefly introduce the Friedmann equations for our model. The observational data to be used, including SNe Ia, BAO and distance priors from CMB, are presented in Section 3. Section 4 contains our main results and some discussion. We conclude in Section 5.

2. Phenomenologically Emergent Dark Energy (PEDE) Model

The Hubble parameter within the Friedmann–Lemaître–Robertson–Walker (FLRW) metric, assuming a flat universe, can be described as

$$H^2(z) = H_0^2[\Omega_m(1 + z)^3 + \Omega_{\rm DE}(z)] \quad (1)$$

where Ω_m is the matter density at the present time, and $\Omega_{\rm DE}(z)$ is dark energy density as a function of redshift z, which can be expressed as

$$\Omega_{\rm DE}(z) = \Omega_{\rm DE,0} \times \exp\left[3\int_0^z \frac{1 + w(z')}{1 + z'}dz'\right] \quad (2)$$

where $w(z) = p_{\rm DE}/\rho_{\rm DE}$ is the equation of state of dark energy.

In the ΛCDM model, $w(z) = -1$ and $\Omega_{\rm DE}(z) = (1 - \Omega_m) =$ constant. For the widely used Chevallier–Polarski–Linder (CPL) parameterization model (w_0–w_a model; Chevallier & Polarski 2001; Linder 2003), the equation of state of dark energy is given by $w(z) = w_0 + \frac{w_a z}{1+z}$ so one can derive $\Omega_{\rm DE}(z) = \Omega_{\rm DE,0}(1+z)^{3(1+w_0+w_a)}\exp\left(\frac{-3w_a z}{1+z}\right)$.

In this Letter, we introduce the PEDE model in which the dark energy density has the following form:

$$\Omega_{\rm DE}(z) = \Omega_{\rm DE,0} \times [1 - \tanh(\log_{10}(1+z))] \quad (3)$$

where $\Omega_{\rm DE,0} = 1 - \Omega_{0m}$ and $1 + z = 1/a$, where a is the scale factor. This dark energy model has no degree of freedom (similar to the case of the ΛCDM model) and we can derive its equation of state following:

$$w(z) = \frac{1}{3}\frac{d\ln\Omega_{\rm DE}}{dz}(1+z) - 1 \quad (4)$$

where we get

$$w(z) = -\frac{1}{3\ln 10} \times \frac{1 - \tanh^2[\log_{10}(1+z)]}{1 - \tanh[\log_{10}(1+z)]} - 1 \quad (5)$$

$$= -\frac{1}{3\ln 10} \times (1 + \tanh[\log_{10}(1+z)]) - 1. \quad (6)$$

Note that in this model, the equation of state of dark energy at early times would be $w(z) = -\frac{2}{3\ln 10} - 1$ and it will evolve asymptotically to $w(z) = -1$ in the far future. In this model we have $w(z=0) = -\frac{1}{3\ln 10} - 1$ at the present for the dark energy. In Figure 1, we can see the behavior of this dark energy model in comparison to Λ. We should note that we can consider a more generalized form of this emergent dark energy model introducing one or more degrees of freedom, such as having $\Omega_{\rm DE}(z) = \Omega_{\rm DE,0} \times \frac{F(z)}{F(z=0)}$ with $F(z) = 1 - \tanh([\log_{10}(1+z) - \log_{10}(1+z_t)])$, where z_t is the transition redshift (similar models have been discussed in Bassett et al. 2002; Shafieloo et al. 2009), but our results show that there is no statistical need to introduce an additional degree of freedom for this model. We can also use this generalized form and set z_t to be the redshift of dark energy matter density equality, where in this case there will not be any additional degree of freedom. The behavior of this generalized form with its self-tuning characteristics will be discussed in future works.

3. Analysis

In order to place constraints on the dark energy models that we have described above, we consider different observations in our work, including the following.

(i) SNe Ia: we use the new "Pantheon" sample (Scolnic et al. 2018), which is the largest combined sample of SN Ia and consists of 1048 data with redshifts in the range $0.01 < z < 2.3$. In order to reduce the impact of calibration systematics on cosmology, the Pantheon compilation uses cross-calibration of the photometric systems of all of the subsamples used to construct the final sample.

(ii) BAOs: four lower-redshift BAO data sets are used. These are the 6-degree Field Galaxy Survey (6dFGS; Beutler et al. 2011), the Sloan Digital Sky Survey (SDSS) Data Release 7 Main Galaxy sample (MGS; Ross et al. 2015), the BOSS Data Release 12 (DR12) galaxies (Alam et al. 2017a), and the eBOSS Data Release 14 (DR14) quasars (Zhao et al. 2019). In addition to these lower BAO measurement, a higher-redshift BAO measurement, which is derived from the cross-correlation of Lyα absorption and quasars in eBOSS DR14, was also used (Blomqvist et al. 2019; de Sainte Agathe et al. 2019).

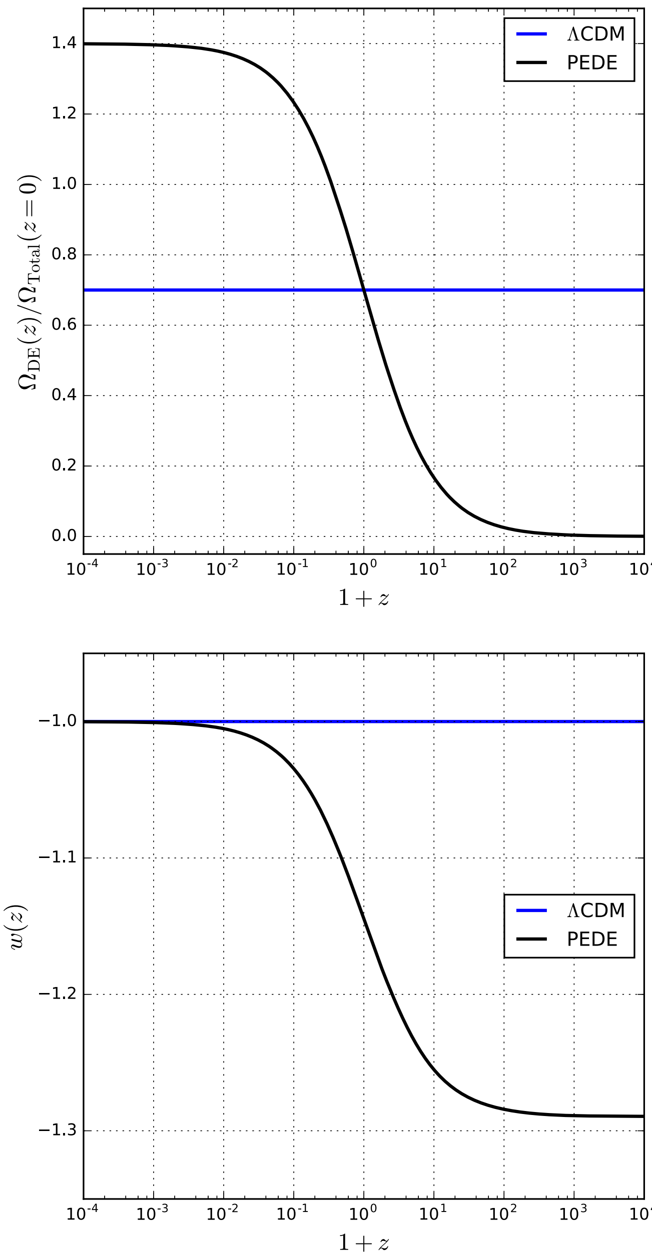

Figure 1. Top panel: the evolution of dark energy density $\Omega_{\rm DE}(z)$ from early times to the far future. Bottom panel: the evolution of the equation of state of dark energy $w(z)$ for ΛCDM and PEDE models. This figure simply demonstrates the behavior of this model in comparison with cosmological constant and flatness, and $\Omega_m = 0.3$ is assumed for both ΛCDM and PEDE models.

(iii) CMB: We include CMB in our analysis by using the CMB distance prior, the acoustic scale $l_{\rm a}$, and the shift parameter R together with the baryon density $\Omega_b h^2$. The shift parameter is defined as

$$R \equiv \sqrt{\Omega_m H_0^2}\, r(z_*)/c \quad (7)$$

and the acoustic scale is

$$l_a \equiv \pi r(z_*)/r_s(z_*) \quad (8)$$

where $r(z_*)$ is the comoving distance to the photon-decoupling epoch z_*. We use the distance priors from the

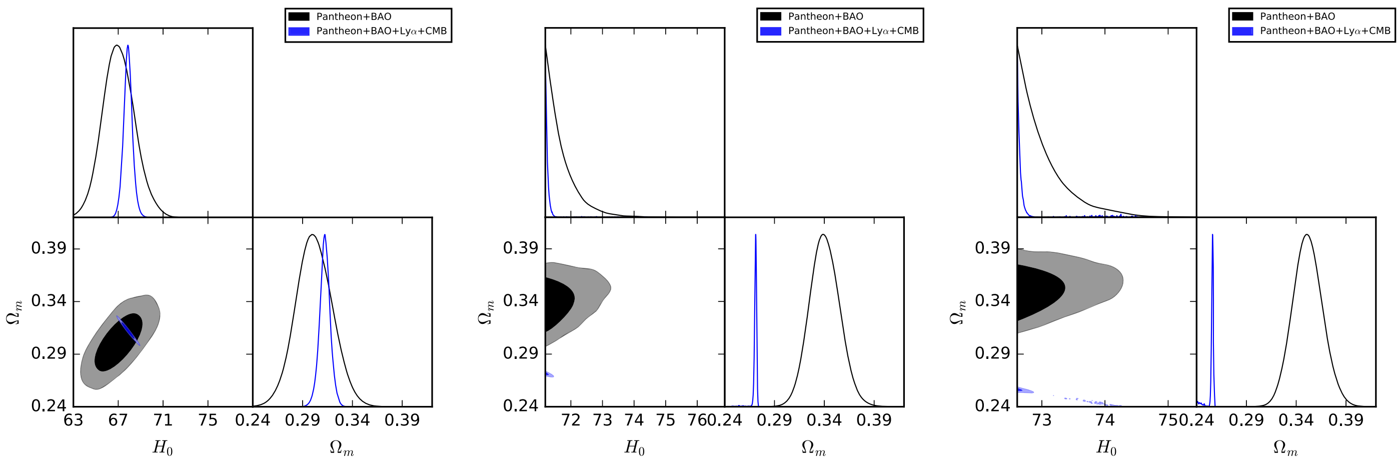

Figure 2. 2D regions and 1D marginalized distributions with 1σ and 2σ contours for the ΛCDM model from different observations. From left to right, we use no H_0 prior, 2σ hard-cut H_0 prior, and 1σ hard-cut H_0 prior from Riess et al. (2019), respectively. The black curves/contours denote for the constraints from Pantheon +BAO, and the blue ones are derived with Pantheon+BAO+Lyα+CMB data combination.

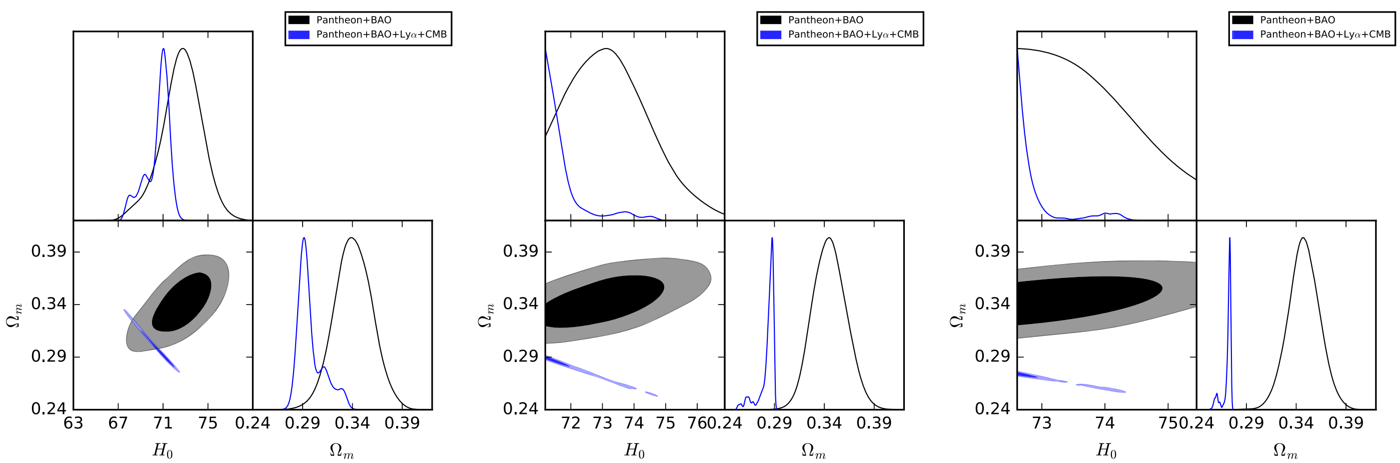

Figure 3. 2D regions and 1D marginalized distributions with 1σ and 2σ contours for the PEDE model from different observations. From left to right, we use no H_0 prior, 2σ hard-cut H_0 prior, and 1σ hard-cut H_0 prior from Riess et al. (2019), respectively. The black curves/contours denote the constraints from Pantheon+BAO, and the blue ones are derived with Pantheon+BAO+Lyα+CMB data combination.

finally release *Planck* TT, TE, EE +low E data in 2018 (Chen et al. 2019), which makes the uncertainties 40% smaller than those from *Planck* TT+low P.

In our analysis, we consider two kinds of data combinations. The first is lower-redshift measurements: the Pantheon supernova compilation in combination with lower-redshift BAO measurements from 6dFGS, MGS, BOSS DR12, and eBOSS DR14 (hereafter referred to as Pantheon+BAO). The second includes higher-redshift observations from Lyα BAO measurements and CMB data (hereafter referred to as Pantheon+BAO +Lyα+CMB). In addition to these data combinations, 2σ and 1σ hard-cut H_0 priors, based on local measurement from Riess et al. (2019) $H_0 = 74.03 \pm 1.42$, are used.

When using SNe Ia and BAO as cosmological probes, we use a conservative prior for $\Omega_b h^2$ based on the measurement of D/H by Cooke et al. (2018) and standard BBN with modeling uncertainties. The constraint results are obtained with Markov Chain Monte Carlo (MCMC) estimation using `CosmoMC` (Lewis & Bridle 2002). For a quantitative comparison between our proposed model, the ΛCDM model and a CPL parameterization, we employ the deviance information criterion (DIC; Spiegelhalter et al. 2002; Liddle 2007), which is defined as

$$\mathrm{DIC} \equiv D(\bar{\theta}) + 2p_D = \overline{D(\theta)} + p_D, \tag{9}$$

where $p_D = \overline{D(\theta)} - D(\bar{\theta})$ and $D(\bar{\theta}) = -2 \ln \mathcal{L} + C$, C is a "standardizing" constant depending only on the data that will vanish from any derived quantity, and D is the deviance of the likelihood. If we define an effective χ^2 as usual by $\chi^2 = -2 \ln \mathcal{L}$, we can write

$$p_D = \overline{\chi^2(\theta)} - \chi^2(\bar{\theta}). \tag{10}$$

We will show that by considering the priors for the Hubble constant, our proposed model can outperform both the ΛCDM model and the w_0–w_a parameterization by comparing their best-fit likelihoods as well as their derived deviance information criterion.

4. Results

We show results for the ΛCDM in Figure 2, in which we present the 2D regions and 1D marginalized distributions with 1σ and 2σ contours from different data combinations. The left panel shows the results with no H_0 prior, and the middle and right panels show the results of setting a hard-cut 2σ H_0 prior

Table 1
Constraints on the Parameters χ^2_{bf} and DIC for the ΛCDM Model, CPL Parameterization, and PEDE Model

Model	Data	Pantheon+BAO			Pantheon+BAO+Lyα+CMB		
	Parameters	No H_0 Prior	2σ H_0 Prior	1σ H_0 Prior	No H_0 Prior	2σ H_0 Prior	1σ H_0 Prior
ΛCDM	Ω_m	$0.299^{+0.047}_{-0.043}$	$0.335^{+0.040}_{-0.036}$	$0.347^{+0.041}_{-0.036}$	$0.311^{+0.016}_{-0.014}$	$0.271^{+0.002}_{-0.003}$	$0.256^{+0.002}_{-0.002}$
	H_0	$66.94^{+3.721}_{-3.256}$	$71.19^{+1.890}_{0.0}$	$72.61^{+1.617}_{-0.000}$	$67.91^{+1.074}_{-1.150}$	$71.19^{+0.271}_{-0.000}$	$72.61^{+0.200}_{-0.000}$
	χ^2_{bf}	1046.94	**1054.76**	**1060.25**	1056.12	**1112.28**	**1168.98**
	DIC	1051.00	**1058.88**	**1064.27**	1062.35	**1127.03**	**1195.07**
CPL	Ω_m	$0.285^{+0.113}_{-0.180}$	$0.332^{+0.071}_{-0.050}$	$0.350^{+0.050}_{-0.043}$	$0.307^{+0.026}_{-0.021}$	$0.286^{+0.007}_{-0.011}$	$0.274^{+0.006}_{-0.009}$
	H_0	$64.84^{+14.49}_{-16.12}$	$71.30^{+5.561}_{-0.117}$	$72.70^{+2.746}_{-0.091}$	$68.49^{+2.302}_{-2.680}$	$71.19^{+1.277}_{-0.002}$	$72.61^{+0.918}_{-0.004}$
	w_0	$-0.82^{+0.193}_{-0.541}$	$-1.08^{+0.422}_{-0.347}$	$-1.05^{+0.350}_{-0.347}$	$-0.98^{+0.267}_{-0.218}$	$-1.07^{+0.259}_{-0.240}$	$-1.13^{+0.274}_{-0.206}$
	w_a	$0.675^{+0.547}_{-3.103}$	$-0.11^{+1.510}_{-3.192}$	$-0.46^{+1.830}_{-2.686}$	$-0.16^{+0.816}_{-1.109}$	$-0.20^{+0.986}_{-1.240}$	$-0.11^{+0.728}_{-1.321}$
	χ^2_{bf}	1044.98	**1048.84**	**1049.66**	1055.52	**1066.85**	**1080.83**
	DIC	1052.59	**1054.46**	**1056.23**	1065.48	**1085.06**	**1128.50**
PEDE	Ω_m	$0.341^{+0.045}_{-0.041}$	$0.341^{+0.041}_{-0.037}$	$0.341^{+0.041}_{-0.030}$	$0.291^{+0.015}_{-0.016}$	$0.289^{+0.002}_{-0.014}$	$0.274^{+0.002}_{-0.006}$
	H_0	$72.84^{+3.814}_{-3.530}$	$73.01^{+3.371}_{-1.8231}$	$72.79^{+2.652}_{-0.186}$	$71.02^{+1.452}_{-1.368}$	$71.19^{+1.306}_{-0.001}$	$72.61^{+0.651}_{-0.000}$
	χ^2_{bf}	1050.04	**1050.04**	**1050.04**	1071.12	**1071.20**	**1080.40**
	DIC	1052.01	**1053.33**	**1052.98**	1091.15	**1091.65**	**1100.94**

Note. Note that with hard-cut H_0 priors, the PEDE model is clearly outperforming the ΛCDM model. With the 1σ hard-cut H_0 prior, the PEDE model is performing even better than the CPL parameterization. Best-fit χ^2 and DIC values for different models assuming H_0 hard-cut priors are bolded for comparison.

and 1σ H_0 prior, respectively. Figure 3 shows the results for our PEDE model. Comparing Figures 2 and 3, we can find that PEDE model pushes the values of both H_0 and Ω_m toward a higher direction for Pantheon+BAO data sets when no H_0 prior is considered. However, adding CMB and high-redshift BAO measurements makes the constraints on value of Ω_m slightly smaller. While the tension in the estimated value of the Hubble Constant is relieved in the PEDE model, some tension in the estimated value of the matter density persists (though substantially reduced in comparison with the case of ΛCDM model).

The parameter constraints for the ΛCDM model, w_0–w_a parameterization, and PEDE model are summarized in Table 1, in which we also show the best-fit χ^2 and DIC values for each model from different data combinations. The χ^2 distributions for the converged MCMC chains for the ΛCDM model, w_0–w_a parameterization, and PEDE model from lower-redshift observations (left panel) and combined observations (right panel) are shown in Figure 4. The upper plots are based on a hard-cut 2σ H_0 prior, and the lower plots are based on a hard-cut 1σ H_0 prior. From Table 1 and Figure 4 we can see that the PEDE model provides substantially better χ^2_{bf} with respect to the ΛCDM model considering 2σ H_0 prior, with $\Delta\chi^2_{bf} = -4.72$ for lower-redshift observations and $\Delta\chi^2_{bf} = -41.08$ for the combined observations. When calculating DIC for different models, we find $\Delta\,\mathrm{DIC} = -5.55$ and $\Delta\,\mathrm{DIC} = -35.38$ with respect to the ΛCDM model for lower redshifts and combined observations, respectively. DIC for the PEDE model is very much comparable with the w_0–w_a parameterization when setting a 2σ H_0 prior.

As can be seen from Table 1 and the lower plots in Figure 4, with the 1σ hard-cut H_0 prior the χ^2_{bf} of the PEDE model becomes much lower than that of the ΛCDM model, with $\Delta\chi^2_{bf} = -10.21$ for lower-redshift observations and $\Delta\chi^2_{bf} = -88.58$ for combined observations. This is comparable with the w_0–w_a parameterization model, which has 2 more degree of freedom. When calculating DIC values, the PEDE model gives the best results among the three models that we considered, with $\Delta\,\mathrm{DIC} = -94.13$ with respect to the ΛCDM model and $\Delta\,\mathrm{DIC} = -27.56$ with respect to the w_0–w_a parameterization for combined observations. The lower plots in Figure 4 clearly show how the proposed PEDE model outperforms the ΛCDM model if we set hard-cut H_0 priors, effectively ruling it out with high statistical significance where the tail of χ^2 distribution for this model has no overlap with the same distribution of the ΛCDM model. We should note that the considered 2σ and 1σ hard-cut priors for the Hubble Constant that effectively affects the assumed models from the lower bound, associated with 97.72% and 84.13% probabilities, respectively. In other words there is a 97.72% chance that our results for 2σ H_0 prior holds with future observations (with higher precision) and there is a 84.13% chance that our results with 1σ H_0 prior holds with future high-precision observations.

5. Conclusion

We propose a simple phenomenologically emergent model of dark energy that has zero degrees of freedom, which is similar to the case of the cosmological constant. The proposed functional form based on a hyperbolic tangent function has a symmetrical behavior in dark energy density as a function of the scale factor in logarithmic scales. The argument behind having the pivot of symmetry at the current time can be associated with the fact that dark energy and matter densities are comparable at the current time. This model can be trivially modified to set the pivot of symmetry at the scale of dark energy dark matter density equality, which would be at $z \approx 0.3$. In our proposed PEDE model, dark energy has no effective presence in the past and its density increases to double its current value in the far future. Theoretically, this will be associated with a dark energy component with $w = -\frac{2}{3\ln 10} - 1$ in the past that will evolve to $w = -1$ in the far future.

Setting hard-cut 2σ and 1σ priors on the Hubble Constant from local measurements associated with 97.72% and 84.13% probabilities, respectively, and using most recent cosmological observations from the low- and high-redshift universe, our

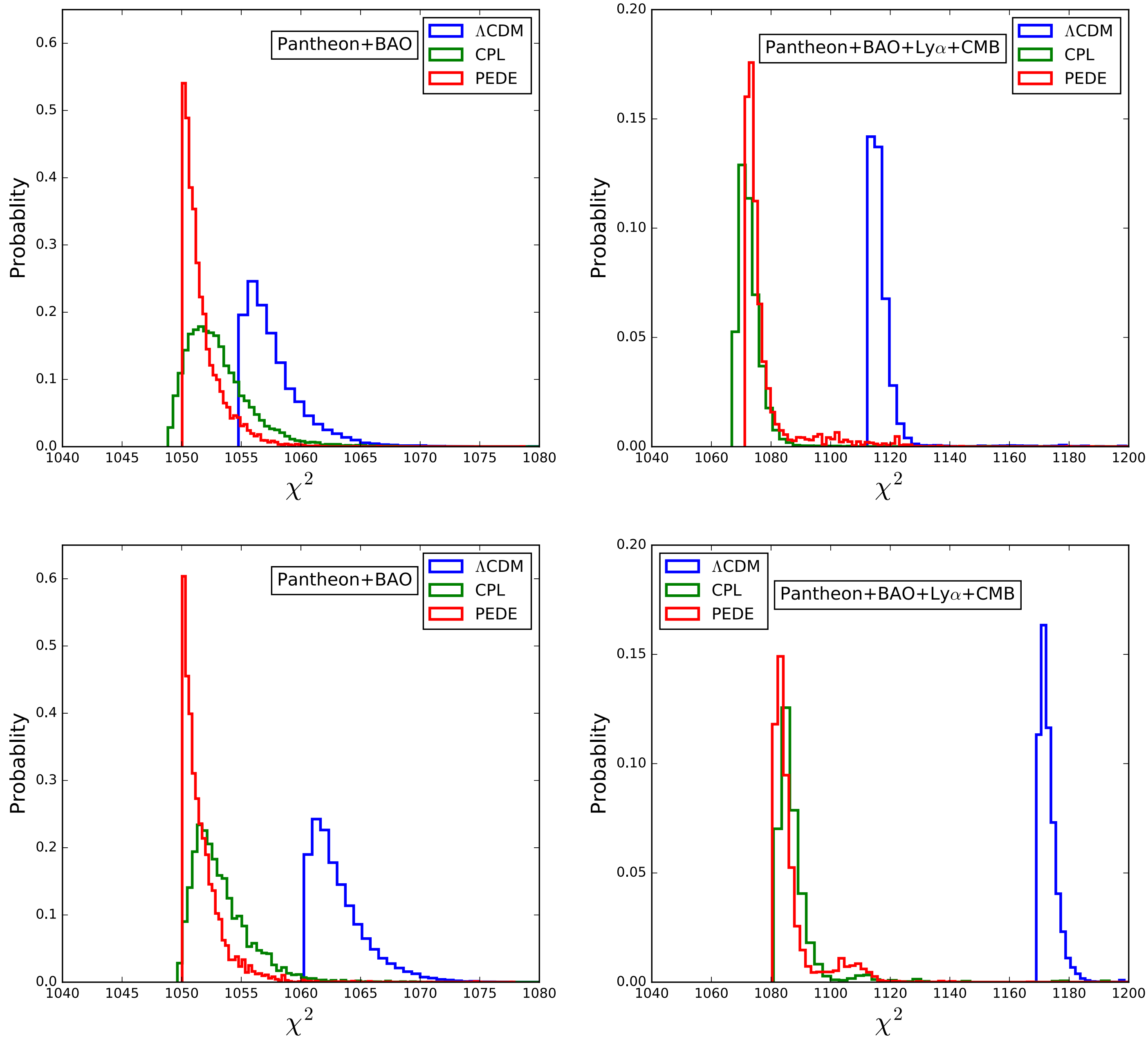

Figure 4. Histograms of χ^2 distribution from the converged MCMC chains for the ΛCDM model, CPL, and PEDE are presented. The left plots show the χ^2 distribution for the Pantheon+BAO combination, and the right plots are obtained with Pantheon+BAO+Lyα+CMB combination. The upper plots are derived by setting the 2σ H_0 hard-cut prior, and the lower plots are derived by setting the 1σ hard-cut H_0 prior. Combining all the data, there is hardly an overlap between the χ^2 distribution of the PEDE model and the ΛCDM model that explains the huge difference that we derived for their DIC.

proposed model surpasses the cosmological constant with large margins. Assuming the reliability of the Hubble Constant measurement and no substantial systematics in any of the data that we used, with 2σ and 1σ hard-cut priors of H_0 our proposed PEDE model rules out the cosmological constant with large statistical significance ($\Delta\,\mathrm{DIC} = -35.38$ and $\Delta\,\mathrm{DIC} = -94.13$, respectively). It is indeed interesting that with the 1σ hard-cut prior on H_0, this model can even outperform the widely used w_0–w_a parametric form with $\Delta\,\mathrm{DIC} = -27.56$. This is important, as our proposed model is a strong alternative to the cosmological constant in the current standard model of cosmology.

With no information on the Hubble Constant, the concordant ΛCDM model seems to be the most favored model. Consequently, all of our results and the conclusion on ruling out Λ is solely and directly associated with the reliability of the Hubble Constant measurement.

While our proposed model can significantly reduce the tensions in the estimation of the cosmological parameters using low- and high-redshift data, some level of tension remains, in particular in the estimation of the matter density. This matter requires further study in order to understand the origin of any discrepancy that persists in any model assumption. More detailed studies are required to compare our proposed model to different cosmological observations that have traces of ΛCDM assumptions in their pipelines. However, it is evident that making more appropriate treatment of different data for our proposed model can only make this model perform better with respect to the ΛCDM model.

Assuming that current cosmological data are all viable, our proposed model is shown to be a better representative of the effective behavior of dark energy in comparison with the cosmological constant. This work can guide theoretical studies of dark energy and our universe in general.

We should recall that our ultimate goal should be to find a theoretical explanation for dark energy or, in a more fundamental approach, for the whole dark sector considering both dark matter and dark energy. We should consider different possibilities and look for the correct theory of gravity; considering dark energy and dark matter as curvature effects or unifying the whole dark sector might be reasonable ways to explain theoretically the observationally supported emergent behavior of effective dark energy (Capozziello et al. 2006; Yang et al. 2019). Distinguishing between physical and geometrical models of dark energy, as well as modified theories of gravity and breaking degeneracies, is in fact a fundamental task in cosmology that might be achievable by cosmography (Shafieloo et al. 2013, 2018; Capozziello et al. 2019). Future observations could shed light on this important problem.

We should note that at the latest stages of this work we became aware of the work of Keeley et al. (2019), which discussed a similar behavior of dark energy but employed a parametric form that has few degrees of freedom similar to what has been introduced earlier in Bassett et al. (2002) and Shafieloo et al. (2009). The simplicity of our phenomenological model with zero degrees of freedom for the dark energy sector and its great performance is the core of our analysis, which allow us to rule out the cosmological constant with large statistical significance when we set hard priors on the Hubble Constant.

X.L. and A.S. would like to acknowledge the support of the National Research Foundation of Korea (NRF-2016R1C1B2016478). X.L. is supported by the Strategic Priority Research Program of the Chinese Academy of Sciences, grant No. XDB23000000. A.S. would like to acknowledge the support of the Korea Institute for Advanced Study (KIAS) grant funded by the Korean government. This work benefits from the high performance computing clusters Polaris and Seondeok at the Korea Astronomy and Space Science Institute. X.L. and A.S. would like to thank Zong-Hong Zhu and Beijing Normal University for the hospitality during the early stages of this work.

ORCID iDs

Arman Shafieloo https://orcid.org/0000-0001-6815-0337

References

Ade, P. A., Aghanim, N., Arnaud, M., et al. 2016, A&A, 594, A13
Aghanim, N., Akrami, Y., Ashdown, M., et al. 2018, arXiv:1807.06209
Alam, S., Ata, M., Bailey, S., et al. 2017a, MNRAS, 470, 2617
Alam, U., Bag, S., & Sahni, V. 2017b, PhRvD, 95, 023524
Bassett, B. A., Kunz, M., Silk, J., & Ungarelli, C. 2002, MNRAS, 336, 1217
Beutler, F., Blake, C., Colless, M., et al. 2011, MNRAS, 416, 3017
Blomqvist, M., et al. 2019, arXiv:1904.03430
Capozziello, S., Cardone, V., & Troisi, A. 2006, JCAP, 2006, 001
Capozziello, S., D'Agostino, R., & Luongo, O. 2019, IJMPD, 28, 1930016
Chen, L., Huang, Q.-G., & Wang, K. 2019, JCAP, 2019, 028
Chevallier, M., & Polarski, D. 2001, IJMPD, 10, 213
Cooke, R. J., Pettini, M., & Steidel, C. C. 2018, ApJ, 855, 102
de Sainte Agathe, V., Balland, C., du Mas des Bourboux, H., et al. 2019, arXiv:1904.03400
Ding, X., Biesiada, M., Cao, S., Li, Z., & Zhu, Z.-H. 2015, ApJL, 803, L22
Hazra, D. K., Shafieloo, A., & Souradeep, T. 2019, JCAP, 2019, 036
Keeley, R. E., Joudaki, S., Kaplinghat, M., & Kirkby, D. 2019, arXiv:1905.10198
Lewis, A., & Bridle, S. 2002, PhRvD, 66, 103511
Liddle, A. R. 2007, MNRAS: Letters, 377, L74
Linder, E. V. 2003, PhRvD, 68, 083503
Riess, A. G., Casertano, S., Yuan, W., Macri, L. M., & Scolnic, D. 2019, ApJ, 876, 85
Riess, A. G., Macri, L. M., Hoffmann, S. L., et al. 2016, ApJ, 826, 56
Riess, A. G., Rodney, S. A., Scolnic, D. M., et al. 2018, ApJ, 853, 126
Ross, A. J., Samushia, L., Howlett, C., et al. 2015, MNRAS, 449, 835
Sahni, V., Shafieloo, A., & Starobinsky, A. A. 2014, ApJL, 793, L40
Scolnic, D., Jones, D., Rest, A., et al. 2018, ApJ, 859, 101
Shafieloo, A., Kim, A. G., & Linder, E. V. 2013, PhRvD, 87, 023520
Shafieloo, A., L'Huillier, B., & Starobinsky, A. A. 2018, PhRvD, 98, 083526
Shafieloo, A., Sahni, V., & Starobinsky, A. A. 2009, PhRvD, 80, 101301
Shanks, T., Hogarth, L., & Metcalfe, N. 2019, MNRAS, 484, L64
Solà, J., Gómez-Valent, A., & de Cruz Pérez, J. 2017, PhLB, 774, 317
Spiegelhalter, D. J., Best, N. G., Carlin, B. P., & Van Der Linde, A. 2002, Journal of the Royal Statistical: Society Series b (Statistical Methodology), 64, 583
Yang, W., Pan, S., Vagnozzi, S., et al. 2019, arXiv:1907.05344
Zhao, G.-B., Wang, Y., Saito, S., et al. 2019, MNRAS, 482, 3497
Zheng, X., Ding, X., Biesiada, M., Cao, S., & Zhu, Z.-H. 2016, ApJ, 825, 17